

Selection of Electrolyte Additive Quantities for Lithium-Ion Batteries Using Bayesian Optimization

Felix Hildenbrand,^{*[a, c]} Felix Aupperle,^[b, c] Gereon Stahl,^[a, c] Egbert Figgmeier,^[a, b, c] and Dirk Uwe Sauer^{*[a, b, c]}

The composition of the liquid electrolyte is a key factor in lifetime performance of lithium-ion batteries. The selection and quantification of additives to the electrolyte is an active field of research. This study focuses on finding the optimal additive combination of fluoroethylene carbonate (FEC) and vinylene carbonate (VC) for NMC622-Graphite cells. The central goal of this work is to accelerate the experimental search in a large search area by using a Bayesian-optimization algorithm to guide the search. Different measurements are used as target

variable such as open-circuit voltage gradient and coulombic efficiency. Consequentially, the capability of these measurements for accelerated lifetime prediction compared to conventional ageing tests by cycling is investigated. The search gathered and confirmed additive combinations with excellent performance after four iterations with a total of 15 additive combinations analyzed. The results of this study give insights into the interaction of VC and FEC with regard to ageing.

Introduction

The design of Lithium-Ion Battery (LIB) is constantly improving with regards to energy density and longevity. One lever for the improvement of LIB with liquid electrolytes is the use of additives in the electrolyte. Additives have been a key focus of the cell improvements in past years.^[1-5] Additives influence the initial solid electrolyte interphase (SEI) formation.^[6] For high surface graphite anode materials, reducing the lithium inventory loss during formation increases the energy density.^[7] Over the lifetime, additives stabilize the SEI under operating conditions, prevent further reaction of the electrolyte with the anode material,^[8] and can suppress transition metal cross-talk.^[9] Continuous formation and reformation of SEI is a key ageing process of LIB, driving loss of lithium inventory and increase of the internal resistance.^[10] Additives have also extended the duration of cycle life before complete loss of capacity due to rollover.^[2] The additives vinylene carbonate (VC) and fluoroethylene carbonate (FEC) are among the most commonly used ones. Both are reported to contribute to the formation of CO₂

(carbon dioxide) which reacts to Li₂CO₃ (lithium carbonate), a key component of the SEI.^[8,11] VC is an established additive in the industry known to be extending cycle life of graphite based anodes.^[12] Burns et al. studied the impact of different amounts of VC, showing that increasing the VC concentration increased cycle life. This was explained by the consumption of VC rather than other electrolyte components such as EC during formation, leaving EC for consumption during cycle life.^[13] It was reported that past a threshold of 4 weight-% (wt%) of VC concentration, the charge transfer resistance increased, reducing the cell performance at higher C-rates.^[2] VC is also reported to increase irreversible capacity loss during formation^[14] and to decrease of coulombic efficiency (CE)^[1,14] leading to the conclusion that the VC concentration should not be too high. This leaves the question: What is the optimal quantity of VC?

Using FEC as an additive has proven to extend cycle life for silicon composed anodes. Intan et al.^[15] showed that adding FEC to the electrolyte leads to a thinner and more flexible SEI. FEC also showed positive effects on cycle life of cells with pure graphite anodes, especially at higher temperatures.^[16,17] Besides the formation of lithium carbonates, FEC also leads to the formation of LiF (lithium fluoride),^[18] which is highly desirable for creating a stable SEI.^[19,20] Burns et al. showed that a combination of VC and FEC can outperform cells which only used one of the two additives with regard to cycle life.^[2] The idea that both additives interact during formation is supported by the findings of Michan et al.,^[21] showing that both additives lead to formation of the same SEI components but in different concentrations. Zhang et al.^[1] points out that there is a possible reaction path from FEC to VC, which makes the interaction of the two additives even more complex.

Considering the results of previous works, we assumed that there is an optimal combination of VC and FEC. Maximum concentrations of additives are indicated in the literature between 5 wt%^[1] and 10 wt%.^[22] Beyond 10 wt%, they are

[a] F. Hildenbrand, G. Stahl, Prof. Dr. E. Figgmeier, Prof. Dr. D. U. Sauer
ISEA RWTH Aachen, Jaegerstr. 17/19, 52066 Aachen, Germany
E-mail: felix.hildenbrand@isea.rwth-aachen.de
dirkuwe.sauer@isea.rwth-aachen.de

[b] F. Aupperle, Prof. Dr. E. Figgmeier, Prof. Dr. D. U. Sauer
Helmholtz Institute Muenster (HI MS), IEK-12, Forschungszentrum Juelich,
Jaegerstr. 17/19, 52066 Aachen, Germany

[c] F. Hildenbrand, F. Aupperle, G. Stahl, Prof. Dr. E. Figgmeier,
Prof. Dr. D. U. Sauer
Juelich Aachen Research Alliance, JARA-Energy, 52062 Aachen, Germany

 Supporting information for this article is available on the WWW under
<https://doi.org/10.1002/batt.202200038>

 © 2022 The Authors. *Batteries & Supercaps* published by Wiley-VCH GmbH.
This is an open access article under the terms of the Creative Commons Attribution Non-Commercial License, which permits use, distribution and reproduction in any medium, provided the original work is properly cited and is not used for commercial purposes.

considered part of the base electrolyte. For concentrations from 0 to 10 wt%, the search space for optimal combination of both electrolytes is very large. Considering 0.05 wt% as smallest increment in concentration that we could have achieved, the number of possible combinations is: $n = 200^2 = 40,000$. Of course this is hypothetical figure, but it illustrates the size of the search space. In order to investigate such vast search spaces systematically, Bayesian optimization has been proven helpful. It is especially suitable in a multivariable search space, where the correlation between input and output variable is unknown.^[23] In comparison to classical design of experiment Bayesian optimization uses a Gaussian Process (GP) rather than a linear function to describe the correlation between the parameters of the search space and the target variable. Guidance in the selection of experiments is especially important when the experiments, as in this case, are costly and time intensive. So it must be ensured that single experiments either contribute to exploration: testing areas where the knowledge is small, or exploitation: improving a known good result. Bayesian optimization is already very present in the field of chemical engineering.^[24,25] Recently, algorithm guided optimization of experiments has been applied to battery electrolyte research. Whitacre et al.^[26] presented a guided search for different additive combinations to improve the electrolyte conductivity. From the same group, Dave et al.^[27] presented an experimental series to improve the electrochemical stability window of electrolytes through selected additives. In both cases the electrolytes were mixed in a fully automated setup and automatically evaluated ex-situ. The results were processed with a framework for Bayesian optimization, guiding the search towards unknown optimal solutions while considerably reducing the experimental effort.

In contrast, this publication aimed at evaluating the electrolytes in-situ, in an operational pouch cell, which didn't allow a fully automated setup. The usage of an algorithms to guide the experimental search required quantitative inputs and outputs of the experiment. While the inputs were simply the two additive concentrations, the quantitative outputs were more difficult to choose. Three methods have been used in the past to evaluate the performance of electrolytes in LIB: the discharge capacity during cyclic ageing,^[17] the CE measured with high-precision coulombmetry (HPC)^[28] and the voltage gradient through open-circuit voltage (OCV) tracking.^[2] The three methods can be performed in very different time ranges and do not have the same significance. Cyclic ageing takes several months, but is the most significant experiment as it relates directly to application of LIB. The investigation of the CE takes one to two weeks. Burns et al.^[2] showed that it allows to predict longterm ageing behaviour. While it is undoubted that the CE is related to parasitic reactions driving the ageing of LIB,^[29] its role as an universal predictor of the ageing performance is not clear.^[30] The measurement of the voltage gradient takes a few days up to a week. It requires the least complex equipment and it is the fastest to perform. That is why it is state of the art as a post production quality control method for LIB. The interpretation of the gradient is less clear. Burns et al.^[2] found consistent results between cyclic ageing, CE and a high voltage gradient.

As the duration of the cell performance evaluation is the bottleneck in the optimization process, the usage of the fastest method is desired. We investigated if and to which extend this is possible. All three evaluation methods have been applied to the samples made in these experiments. The cycling ageing was taken as benchmark as it is most relevant for the application, it was complement by the average discharge voltage as a proxy value for the cell resistance. This allowed to compare the different methods and to evaluate which one is the most suitable for the algorithm used in the optimization. The experiments were performed in four iterations. The results of the previous iterations were used to decide on the selected experiments in the next iterations. A total of 15 additive combinations were investigated.

Results and Discussion

Selection of experiments

After producing the cells of the first iteration the voltage gradient was the first available value. As a smaller gradient had proven to be an indicator for better performance.^[2] To select the experiments of the second iteration the algorithm was trained to minimized the gradient (in absolute value). For this target variable, Figure 1a displays the expectation calculated by the GP in a 2D-plot.

For the selection of the experiments of the third iteration results of the cyclic ageing were available. While the selected value by the algorithm showed a much smaller voltage gradient, it didn't show the expected good cyclic performance. We concluded that the minimization of the voltage gradient was not correlating with good cyclic performance, hence it was not an appropriate indicator for improving the cyclic performance. Table 1 shows the suggestions after two iterations for different optimization parameters. The best performing combination having the highest gradient, except for an outlier, we selected the experiment proposed with the gradient maximization as optimization criteria (Figure 2a). The outlier was excluded from further training. Additionally the GP was trained with the relative capacity at 100 cycles (Figure 2f). The experiment proposed for the CE maximization as an optimization criteria was discarded for being to close to the bad performing 10 wt% FEC, 0 wt% VC.

Table 1. Proposed experiments by the optimization algorithm

Training data Iter. n°	Opti. Parameter	FEC [wt %]	VC [wt %]
1,2	Volt. Grad. Max.	2.29	7.47
1,2	Volt. Grad. Min.	1.85	1.09
1,2	CE Max.	9.1	0
1,2	Rel. Cap. @100 Cyc. Max.	1.61	1.97
1–4	Volt. Grad. Max.	10	5.8
1–4	Volt. Grad. Min.	4.3	9.4
1–4	CE Max.	2.4	1.8
1–4	Init. Abs. Cap. Max.	2.1	0
1–4	Abs. Cap. @400 Cyc. Max.	2.1	0
1–4	Avg. Dch. Volt. @400 Cyc. Max.	0.1	2.5

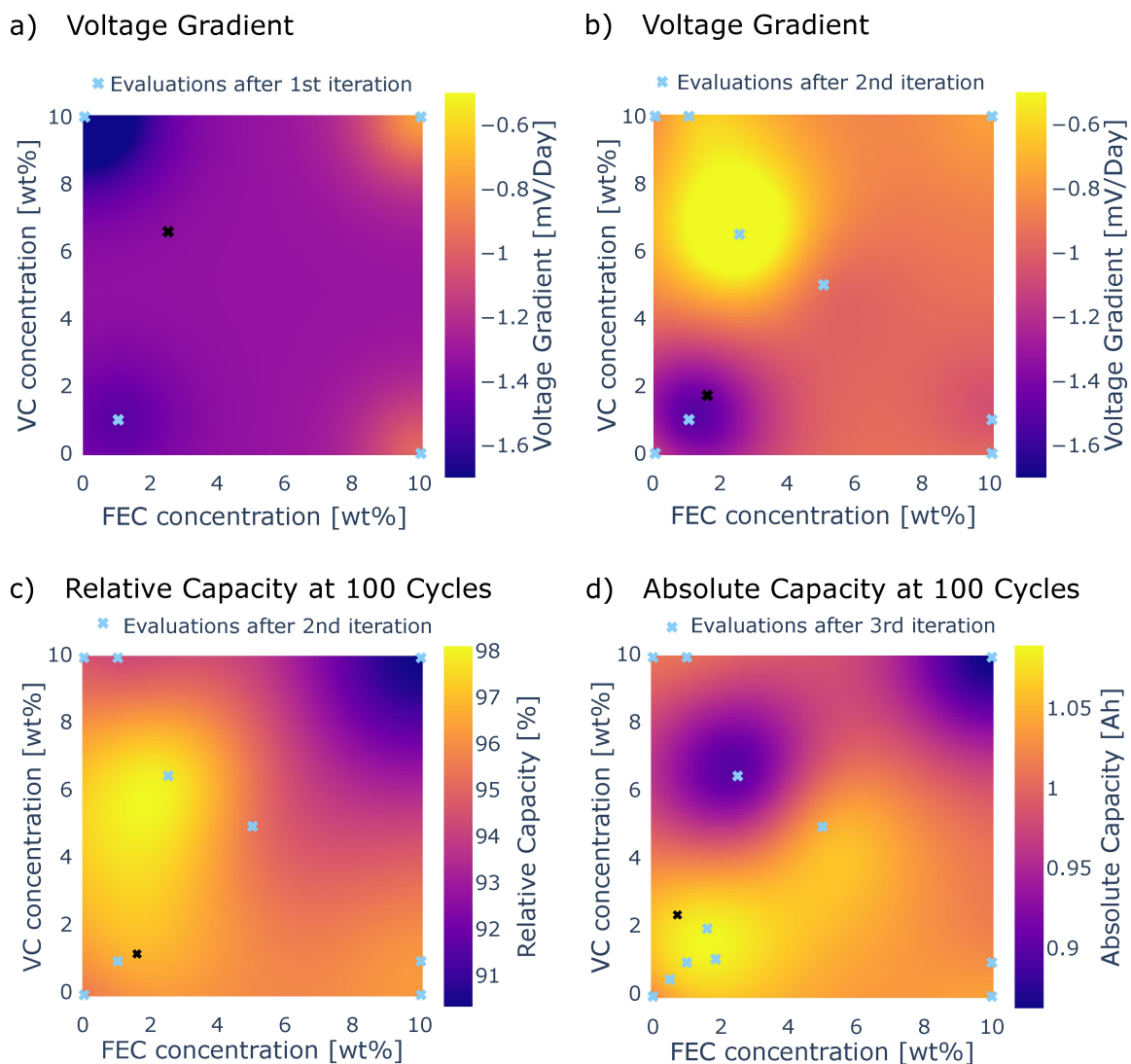


Figure 1. Expectancy of different target variables in the search space, describing the a-priori-knowledge before each of the four proposed experiments. The x- and y-axis indicate the concentrations of the additives, the color the estimated value of the target variable. The position of the training values are indicated by blue crosses. The next experiment proposed by the algorithm is indicated by a black cross.

For the fourth iteration the optimization was done with regard to the absolute capacity rather than the relative as some experiments showed a strong initial decrease in capacity during the formation. This was due to high consumption of active lithium during the formation and in the first cycles, before stabilizing during further cycling. The combination J-3 was repeated to confirm the outperforming results. The GP was retrained a last time after the fourth iteration. The results are displayed in Table 1. Absolute capacity and average discharge voltage at 400 cycles were included as training target values for longterm ageing performance. Considering the low correlation coefficient between the voltage OCV gradient and the long-term performance (see Figure 3) the proposed experiments for minimizing and maximizing the gradient were discarded. The remaining proposed experiments were in an area that was already well covered by the previous experiments (see Figure 1d). At this point the cycling of the two best performing additive combination of 1.85 wt% FEC, 1.1 wt% VC and 1.0 wt%

FEC, 1.0 wt% VC had already reached over 1000 cycles and retained a median capacity of 992 mAh and 1004 mAh, respectively. We concluded that there was little room for improvement to be gained with respect to performance and that the optimization was completed.

Predictive ability of target variables

The delay with which a measurement is available after the electrolyte filling is the biggest lever in reducing the iteration time of the optimization. We analysed the capability to predict the final cell performance of five measurements available within 25 days after the electrolyte filling. Figure 3 shows the correlation between the measurements and the longterm performance indicators. The indicated correlation coefficient r is a Spearman's rank correlation coefficient, it was chosen as it is more robust with regard to outliers. In order to identify

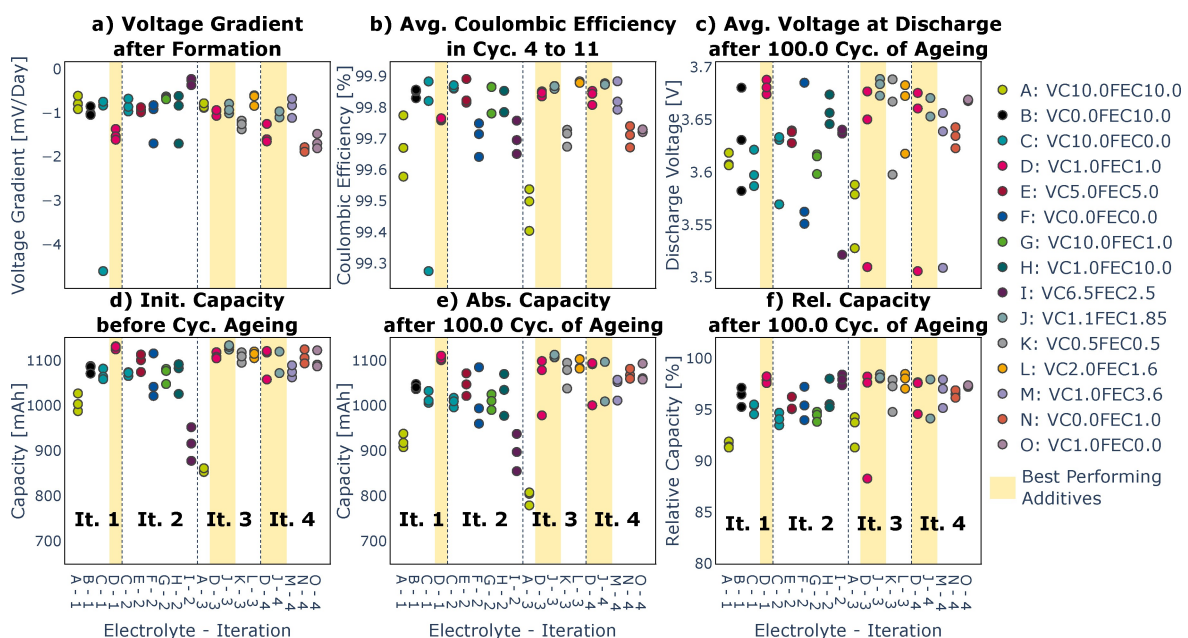


Figure 2. Plot of the investigated parameters in chronological order for each electrolyte sorted by iteration. All measurements were done at 35 °C.

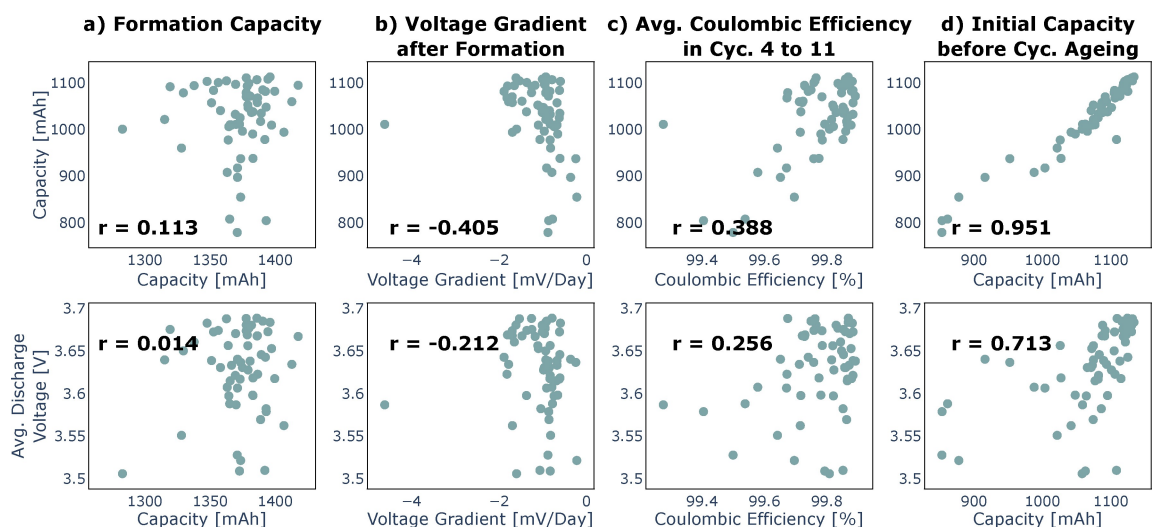


Figure 3. Correlation between capacity and avg. discharge voltage after 400 cycles and measurements at early life. The measurements are sorted from left to right in their order of appearance.

potential target variables for future optimization, we added the initial capacity and the formation capacity. The charged capacity during formation (Figure 3a) showed a very weak correlation. The voltage gradient (Figure 3b) and the CE (Figure 3c) have shown a good prediction capability in previous publications.^[2] But the correlation between these two early measurements and the aged capacity at 400 cycles were not as strong as expected. A similar weak correlation between the ageing performance and the CE was reported by Weng et al.^[30] In our case the initial capacity (Figure 3d) of the cyclic ageing was the best indicator for the longterm performance. The initial capacity was measured after the cells performed eleven full cycles on the HPC, when the capacity loss due to formation

and post formation was completed. This conclusion was underlined by the experiments suggested by the algorithm based on the first four iterations (see Table 1). The next proposed experiments based on the capacity after 400 cycles and on the initial capacity were the same. We concluded that in this case no additional knowledge was gained from 2.5 months of cycling. Hence, in order to increase the speed of development, the first choice for the target variable is to use the initial capacity followed by the CE.

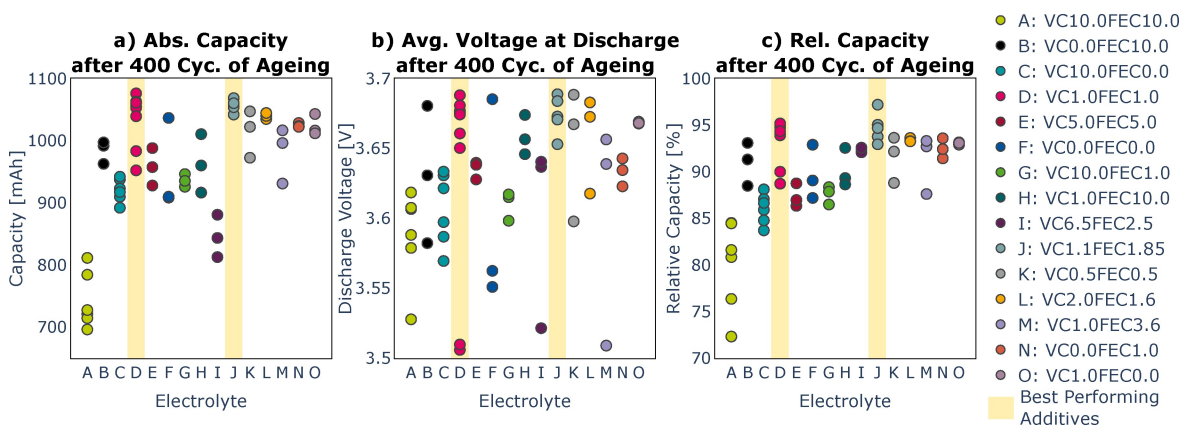


Figure 4. Longterm performance after 400 cycles. Capacity, avg. discharge voltage and rel. capacity sorted by additive combinations.

Performance

The main goal of the selection of electrolyte additives quantities was to improve the cyclic life. Figure 2 displays the performance tests sorted by iterations and Figure 4 the long-term performance at 400 cycles, which was the ageing reached by the latest iteration. Even if some compositions showed higher spread or outliers, performance differences between the different additive compositions were well defined. For the combination J-4 one cell was destroyed before cycling started, therefore results for two cells were available. Between the iterations the performance of the same electrolyte composition, reproduced for reference purposes, were not exactly identical. This was especially pronounced for the voltage gradient. It systematically increased from iteration 2 to 4. The differences between the iterations could be due to small difference in the preparation and in the handling of the cells before the ageing experiment. But within the same iteration the performance differences were consistent.

The two additive combinations D and J outperformed the other combinations in longterm performance throughout two, respectively, three repetitions. Generally, we observed that smaller quantities of additives lead to higher initial capacity, smaller over potentials, and better longterm performance. All combinations with more than 1000 mAh of remaining capacity had less than 5 wt% of each additive, except for the cells without additives. The cells with higher wt% of additives had a higher initial capacity loss or a stronger decrease, leading to a capacity decline below 1000 mAh before 400 cycles. This was also reflected in the experiments selected by the algorithm, most of it in areas with concentration below 4 wt%. The minimum for improving performance lied at 1 wt%. The cells with 0 wt% or 0.5 wt% performed below the top performing combinations.

To better understand the effect of VC and FEC we evaluated the average discharge voltage of one cycle vs. the discharge voltage of this cycle for the cells with 1 wt% of only one of the two additives, displayed in Figure 5. The difference between the electrolytes was significant. The cells filled with VC had a higher avg. discharge voltage for the same capacity than cells

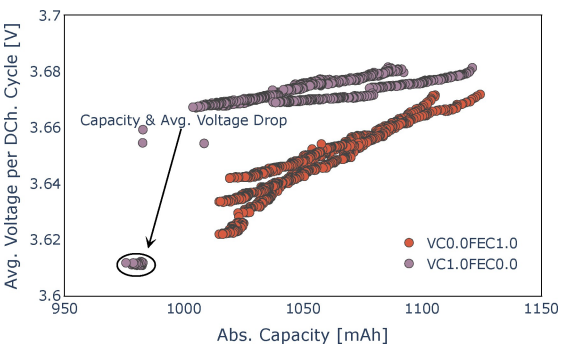


Figure 5. Comparison of the avg. discharge voltage and the capacity for small additive quantities in the 4. iteration., for the first 400 cycles. Each point is a cycle.

filled with FEC, meaning that the cell with VC had smaller over potentials, hence a smaller impedance compared to the cells filled with FEC. This confirms previous results^[12] and is consistent with the EIS measurements of Burns et al.,^[2] where the half circle is smaller for VC compared to FEC. This was not true for higher concentrations of VC (see Figure 4). The additive combinations with 10 wt% VC and a small amount of FEC (C,G) had systematically higher overpotentials and lower capacity after 400 cycles than their counterparts with low VC concentration of 1 wt% (O,D). This was also consistent with earlier findings, which showed an increased over potentials for concentrations of VC over 4.5 wt%.^[2] The comparison between low and high concentration for FEC (N,D vs. B,H) showed a small but much less significant deterioration, from low to high FEC concentration, in the overpotential and the capacity after 400 cycles than for VC. We concluded that a higher FEC concentration has no negative impact on the cell performance while there is a limit for the VC concentration.

The cells prepared in the iterations 1 and 2 had reached over 2000 cycles by the end of the investigation as shown in Figure 6. We observed that cells with a VC concentration of 10 wt% performed significantly worse than cells with a smaller VC concentration. All of the cells that experienced a total loss of capacity by rollover had 10 wt% VC. For the cells with a VC and a FEC concentration of 10 wt% the early rollover after less

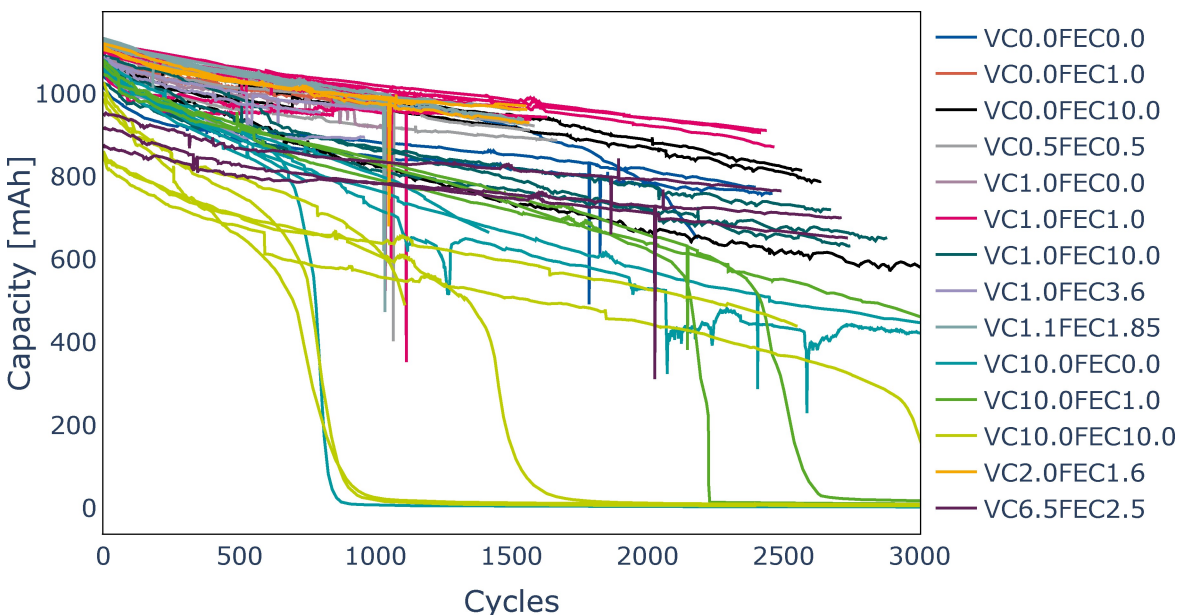


Figure 6. Discharged capacity over cycles for all investigated LIBs. The cycling was performed at 35 °C and cells were symmetrically charged and discharged with a 0.5 A constant-current between 3–4.35 V.

than 1000 cycles could be caused by the reduced concentration in conductive salt. The conductive salt was present in the baseline electrolyte, but it was not increased after the introduction of the additives. The other cells prepared with 10 wt% VC still experienced rollover or showed a strong capacity loss while the cells with 10 wt% FEC, with the same salt concentration, were stable for over 2000 cycles. The cells with a VC concentration of 6.5 wt%, were also stable even though they experienced a strong initial loss. We concluded that a VC concentration of above 6.5 wt% is harmful for the longterm stability of the cell. This is consistent with the results of Yamaguchi et al.,^[31] which observed a deterioration of cell performance for a VC concentration of above 10 wt%. We could not verify the trend observed by Burns et al.^[2] which showed an increase in number of cycles before rollover for an increasing concentrations of VC up to 6 wt% for a similar system. But our data did also not reject this observation as only cells with a VC concentration of 10 wt% experienced a rollover, while all others cell are still operational.

Many of the prepared cells experienced sharp drops and sometime consequent rises of the capacity during cycling (see Figure 6). In Figure 5 the effect of such capacity drop and its related effect on the cells average discharge voltage, which also drops. While it is plausible that the average voltage changes over the ageing due to changing cell balancing, neither such a sharp drop, nor the fact that in some the capacity loss was reversible can be explained by normal degradation. We excluded measurement errors as a source of this disturbance. Micro-short circuits as cause for the drops were also excluded, as the capacity loss was reversible. We concluded that an increase of the overvoltage due to an increase of the cell impedance was at the origin of the capacity drop. We found that the only plausible explanation for a strong

rise in the internal resistance within one cycle was the decontacting of the electrode sheets, triggered by gassing. As the cells were not braced during cycling, the gas was able to expend and evolve through the cell stack.^[32] This would also explain the reversibility of the capacity loss. Gas can be created at the cathode and subsequently reduced at the anode.^[33,34] All cells showed strong capacity drops and rises had 10 wt% of VC with different quantities of FEC. Further we observed that after the rollover, the cells filled with 10 wt% FEC and 10 wt% VC inflated due to gassing. We concluded without further proof, that the gassing was linked to the high VC content.

Conclusion

This work aimed at determining the optimal combination of the electrolyte additives VC and FEC for a NMC/graphite chemistry to improve cycle life. The iterative search for the optimal combination was guided by a GP. Within three iterations two optimal combinations could be determined and their performance was confirmed in a fourth iteration. We showed that a search for an optimal combination of both additives is not trivial. Using a GP to guide the search helped accelerate the search and allowed to select the combination of 1.85 wt% FEC and 1.1 wt% VC, which otherwise would not have been found. The evaluation of the target variables led to the conclusion that the initial capacity was the estimator with the best predictive ability for the longterm performance. While it was not used for the optimization in this work, it should be retained for future works. We observed that additive quantities below 5 wt% of each additive performed better than above 5 wt%. Hence, when optimizing a combination of VC and FEC the search should focus on this smaller search space. The

investigation showed that VC helps to reduce initial capacity loss and overvoltage increase while FEC improves longterm stability. We also found that the concentration of VC should be limited due to its negative impact on longterm stability and gassing behaviour. At the same time, an increased FEC concentration had on the one hand no drawbacks but on the other hand did not further improve the performance. Hence, the amount of used additive could be reduced, which might contribute to reduce costs. The optimization under the constrain of minimizing the used additive quantity could be a starting point for future work. The presented results are a fine tuning for a very specific test scenario. Future work could diversify the test conditions and perform application specific tests, the results of which could be processed in a multi-objective optimization. By this means a purpose design of the additives could be achieved. In general, the presented method could be applied to other cell design parameters known or suspected to affect the lifetime performance. The experimental results could be improved by formalizing or automatizing the sample preparation and the testing process. This would further accelerate the process and increase reproducibility. Finally, an application of parameter selection with Bayesian optimization to an industrial battery production line seems possible and of great interest.

Experimental Section

Preparation of electrolyte solutions

All investigated electrolytes consist of 1.0 M lithium hexafluorophosphate (LiPF₆) dissolved in a mixture of ethylene carbonate (EC) and dimethyl carbonate (DMC), (1:1, v:v) as baseline, and in mixtures with electrolyte additives of FEC and VC by weight. All electrolyte components were obtained from Solvionic and used without further purification. High quality and battery grade baseline (99.9% purity), FEC (99.9%), and VC (99.9%). The electrolyte mixtures were prepared and stored inside an argon-filled glove box (O₂ and H₂O # < 0.5 ppm). Three cells were prepared for each electrolyte sample.

Pouch cell design

1 Ah sealed and dry machine wound pouch cells were obtained from Li Fun Technology Co., Ltd. The ratio of the first lithiation capacity of the negative electrode and first delithiation capacity of the positive electrode of the pouch cells was 1.19 (i.e., N/P, negative/positive). This configuration ensured that no lithium plating would occur at the highest upper cut-off voltage UCV of 4.35 V. The composition of the negative electrode is 94.8% artificial graphite, 1.4% conductive carbon, and 3.8% binder. The positive electrode is 94.0% NMC622, 4.0% conductive carbon, and 2.0% binder. Investigations with an scanning electron microscope (SEM) showed that the particles of the positive electrode were composed of single crystals, similar to the material presented in.^[35]

Electrolyte filling, formation, and cycling protocols

The pouch cells were first opened inside an argon-filled glove box (LABstar, MBRAUN) with an proper inert atmosphere (O₂ and H₂O < 0.5 ppm), followed by drying at 80°C for at least 12 hours.

Thereafter, the pouch cells were filled (by weight) with the electrolyte mixtures. For this doing, the cells were placed on a high precision scale (MSA3203P-100 DU, Sartorius AG) and were filled with 4.5 g of electrolyte solution. To accelerate and guarantee proper wetting of the active materials and separator with electrolyte solution and thereby removing residual gases out of the pores, the electrolyte injected pouch cells were transferred to an airlock. Here, a negative pressure of -0.6 atm was applied for 20 seconds. Afterwards the pouch cells were vacuum-sealed with a vacuum sealing machine (MSK-115A, MTI KJ Group).

For the formation, pouch cells were clamped between two metal plates and a pressure of 0.8 MPa was applied by four screws with special attention not to short circuit the cells. The clamped pouch cells were placed in an oven at 80 °C (UFE 500, Memmert GmbH + Co. KG). After a resting time of 8 hours at OCV, which ensures a complete wetting of the active materials and separator by the electrolyte solution of the pouch cells, the protocol of the formation was as follows: pouch cells were charged once with a constant current of 0.2 C to 4.35 V UCV without constant voltage phase and discharged with constant current of 0.2 C to 3.9 V. Thereafter, the pouch cells were taken back to an argon-filled glove box, in which they were opened and resealed under vacuum in order to remove any gas formed during the formation step.

Testing methods

The electrical tests after the formation were performed in an oven (UFE 500, Memmert GmbH + Co. KG) at 35 °C. After the formation, the cells underwent successively three testing methods. First the OCV was measured for 3 to 10 days. The voltage was automatically measured every 2 hours. In between the measurements, the cells were electrically disconnected from the measurement device by a relay, in order to insure no discharge through the measurement circuit was possible. The time gradient of the voltage was calculated from the voltage time series. The voltage gradient values were used in the following to evaluate the cells performance.

It followed a HPC measurement using a Novonix UHPC 2 A. The pouch cells were cycled in the potential range of 4.35-3 V with a C-Rate of C/20, for 11 to 13 Cycles. To avoid the low CE due to post formation in the first cycles, the cell performance was evaluated from the average coulombic efficiency of cycles 4 to 11. After the cycling for HPC the cells were stored again for 5 to 10 days at 35 °C and 3.0 V before the cyclic ageing was started.

The pouch cells were cycled in the full potential rang of 4.35-3 V with a constant current charge and constant-current discharge protocol using a Neware BTS (CT-ZWJ-4S-1-1U). Cells were symmetrically charged and discharged with a 0.5 A (~0.5 C) constant-current. No resting time and no constant-voltage phase were applied. The cells were cycled without pressure. Absolute capacity and capacity relative to the first cycle at cycle 100 and at cycle 400 were used to evaluate the performance. For each discharge cycle the average voltage was calculated. The average was calculated with regard to time, which was equivalent to electric charge at constant current.

Selection of experiments and optimization

To enhance the search for the optimal additive composition bayesian optimization or kriging was used to select the experiments. As a functional connection between the concentrations of the additives $x = (c_{FEC}, c_{VC})^T$ and the ageing performance is unknown, bayesian optimization substitutes the connection by a GP. A GP can be described as a distribution of functions connecting

the input variables and the output variable of the experiment, it is written as:

$$f(x) \sim GP(m(x), \kappa(x, x')) \quad (1)$$

With the mean function $m(x)$ being the first moment $E[f(x)]$ and the covariance function $\kappa(x, x')$ being the second moment $E[(f(x) - m(x))(f(x') - m(x'))]$. In this case, the GP was used with a zero mean function leaving the covariance function for regression. The covariance functions describes the smoothness of the target variable. The covariance function (or kernel) Matérn 5/2 was chosen according to the recommendation by Snoek et al.^[36] Snoek favored the Matérn kernel over the common choice of the squared exponential kernel for it has less strict smoothness. The GP was trained with tuples of VC and FEC concentrations (0–10 wt%) as input or predictor variables and one of the measurement results (voltage gradient, CE and absolute or relative capacity at cycle 100) was used as dependent or target variable. All values were normalized to values between 0 and 1. The mean of the measurement values of each concentration tuple was taken as target variable in the training while the variance of the measurement values was added as noise to the covariance.

With the GP trained by the a-priori-knowledge of the previous experiments the next experiments could be chosen to maximize the target value (exploitation) or to minimize the unknown (exploration). For this end, three algorithms could be used: the upper confidence bounds method (UCB), the expected improvement method (EI), or the probability improvement criterion (POI). POI was dismissed due to its slower convergence.^[36,37] UCB allowed to guide the suggestion through a parameter, either in direction of improvement or in direction of exploration. This would have required further tuning of the parameter so EI was chosen, as it was the best compromise between improvement and exploration. The suggestion had a random character, as it often the case with algorithmic search, leading to changing results when the algorithm was run a few times in a row. To cope with fluctuating results, the execution of the selection algorithm was repeated 100 times. In all cases over 70 out of 100 results were the same tuple, which was then selected. The complete algorithm is presented by Snoek et al.^[36] For this publication it was used in its python implementation.^[38]

To create and increase the prior knowledge used to train the GP, the search was done in four iterations. Each iteration composed of

Table 2. Selected additive combinations for experiment. Experiment with reference or exploration as motivation were human selected, all other experiments were selected by the algorithm.

Iteration n°	FEC [wt%]	VC [wt%]	Motivation	ID
1	10	10	Exploration	A1
1	10	0	Exploration	B1
1	0	10	Exploration	C1
1	1	1	Exploration	D1
2	5	5	Exploration	E2
2	0	0	Exploration	F2
2	1	10	Exploration	G2
2	10	1	Exploration	H2
2	0	10	Reference (Outlier)	C2
2	2.5	6.5	Minimizing OCV Gradient	I2
3	1.85	1.1	Maximizing OCV Gradient	J3
3	1	1	Reference (Best Iter. 1)	D3
3	0.5	0.5	Exploration	K3
3	10	10	Reference (Worst)	A3
3	1.6	2	Maximizing rel. cap. at 100 cycles	L3
4	3.6	1.1	Maximizing abs. cap. at 100 cycles	M4
4	1	1	Reference (Best Iter. 1)	D4
4	1	0	Exploration	N4
4	0	1	Exploration	O4
4	1.85	1.1	Reference (Best Iter. 3)	J4

three to five additive combinations, called experiments, listed in Table 2. The experiments of the first iteration allowed to explore and delimit the search space, hence additive concentrations at the edges were selected. In the following iterations were prepared: reference experiments to insure reproducibility, human selected exploration experiments and machine selected experiments. The combination of machine selected and human selected experiments has also recently been discussed by Wang et al.^[25] Before each experiment selection the GP was retrained with the results of all previous iterations, leading to an effect of reinforced learning. As displayed in Figure 7, the knowledge about the search space grows through a combination of human and machine selected experiments. The knowledge in the GP can be visualized for a two dimensional search space by plotting the expectation (see Figure 1) and its confidence interval (see Figure A1 in Supporting Information).

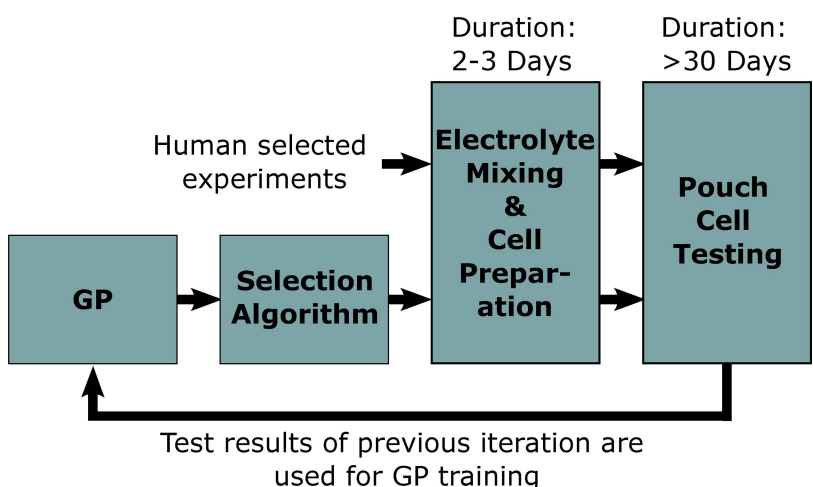


Figure 7. Flowchart describing the experimentation process. The executed experiments are a combination of human selected and machine selected ones.

Author contribution

Author contributions F.H.: Conceptualisation, Methodology, Formal Analysis, Data Curation, Software, Writing – Original Draft Preparation, Visualisation. F.A.: Conceptualisation, Methodology, Investigation, Writing – Original Draft Preparation. G.S.: Methodology, Investigation, Data Curation, Writing – Review and Editing. E.F.: Conceptualisation, Supervision, Resources, Funding Acquisition, Writing – Review & Editing. D.U.S.: Supervision, Funding Acquisition, Writing – Review & Editing.

Acknowledgments

The authors gratefully acknowledge the financial support by Federal Ministry of Education and Research through the projects BALd (BMBF 03XP0320A), E-FloA (BMBF 03XP0349A-B), Meet HiEnD II (BMBF 03XP0084B) and by Engie. The authors specially thank Felix Weber, Sebastian Klick and Martin Graff for the fruitful scientific discussions. F.H. thanks Artur Schweidtmann for introducing him to Bayesian optimization. Open Access funding enabled and organized by Projekt DEAL.

Conflict of Interest

The authors declare no conflict of interest.

Data Availability Statement

The data that support the findings of this study are available from the corresponding author upon reasonable request.

Keywords: ageing · electrolytes additives · gaussian process · lithium-ion batteries · machine learning

- [1] S. S. Zhang, *J. Power Sources* **2006**, *162*, 1379–1394.
- [2] J. C. Burns, A. Kassam, N. N. Sinha, L. E. Downie, L. Solnickova, B. M. Way, J. R. Dahn, *J. Electrochem. Soc.* **2013**, *160*, A1451–A1456.
- [3] D. Y. Wang, N. Sinha, R. Petibon, J. Burns, J. Dahn, *J. Power Sources* **2014**, *251*, 311–318.
- [4] R. Petibon, J. Xia, L. Ma, M. K. G. Bauer, K. J. Nelson, J. R. Dahn, *J. Electrochem. Soc.* **2016**, *163*, A2571–A2578.
- [5] X. Ma, J. E. Harlow, J. Li, L. Ma, D. S. Hall, S. Buteau, M. Genovese, M. Cormier, J. R. Dahn, *J. Electrochem. Soc.* **2019**, *166*, A711–A724.
- [6] E. Peled, *J. Electrochem. Soc.* **1979**, *126*, 2047–2051.
- [7] J. Kasnatscheew, T. Placke, B. Streipert, S. Rothermel, R. Wagner, P. Meister, I. C. Laskovic, M. Winter, *J. Electrochem. Soc.* **2017**, *164*, A2479–A2486.
- [8] E. Peled, S. Menkin, *J. Electrochem. Soc.* **2017**, *164*, A1703–A1719.
- [9] S. Klein, P. Harte, S. van Wickeren, K. Borzutzki, S. Röser, P. Bärmann, S. Nowak, M. Winter, T. Placke, J. Kasnatscheew, *Cell Reps Phys. Sci.* **2021**, *2*, 100521.
- [10] J. Vetter, P. Novák, M. Wagner, C. Veit, K.-C. Möller, J. Besenhard, M. Winter, M. Wohlfahrt-Mehrens, C. Vogler, A. Hammouche, *J. Power Sources* **2005**, *147*, 269–281.
- [11] K. U. Schwenke, S. Solchenbach, J. Demeaux, B. L. Lucht, H. A. Gasteiger, *J. Electrochem. Soc.* **2019**, *166*, A2035–A2047.
- [12] D. Aurbach, K. Gamolsky, B. Markovsky, Y. Gofer, M. Schmidt, U. Heider, *Electrochim. Acta* **2002**, *47*, 1423–1439.
- [13] Y. Wang, S. Nakamura, K. Tasaki, P. B. Balbuena, *J. Am. Chem. Soc.* **2002**, *124*, 4408–4421.
- [14] D. Xiong, J. C. Burns, A. J. Smith, N. Sinha, J. R. Dahn, *J. Electrochem. Soc.* **2011**, *158*, A1431.
- [15] N. N. Intan, J. Pfændtner, *ACS Appl. Mater. Interfaces* **2021**, *13*, 8169–8180.
- [16] I. A. Profatilova, S.-S. Kim, N.-S. Choi, *Electrochim. Acta* **2009**, *54*, 4445–4450.
- [17] M.-H. Ryou, G.-B. Han, Y. M. Lee, J.-N. Lee, D. J. Lee, Y. O. Yoon, J.-K. Park, *Electrochim. Acta* **2010**, *55*, 2073–2077.
- [18] M. Nie, D. P. Abraham, Y. Chen, A. Bose, B. L. Lucht, *J. Phys. Chem. C* **2013**, *117*, 13403–13412.
- [19] V. A. Agubra, J. W. Fergus, *J. Power Sources* **2014**, *268*, 153–162.
- [20] K. H. Kim, J. H. Cho, J. U. Hwang, J. S. Im, Y.-S. Lee, *J. Ind. Eng. Chem.* **2021**, *99*, 48–54.
- [21] A. L. Michan, B. S. Parimalam, M. Leskes, R. N. Kerber, T. Yoon, C. P. Grey, B. L. Lucht, *Chem. Mater.* **2016**, *28*, 8149–8159.
- [22] K. Xu, *Chem. Rev.* **2014**, *114*, 11503–11618.
- [23] B. Shahriari, K. Swersky, Z. Wang, R. P. Adams, N. de Freitas, *Proc. IEEE* **2016**, *104*, 148–175.
- [24] B. J. Shields, J. Stevens, J. Li, M. Parasram, F. Damani, J. I. M. Alvarado, J. M. Janey, R. P. Adams, A. G. Doyle, *Nature* **2021**, *590*, 89–96.
- [25] Y. Wang, T.-Y. Chen, D. G. Vlachos, *J. Chem. Inf. Model.* **2021**, *61*, 5312–5319.
- [26] J. F. Whitacre, J. Mitchell, A. Dave, W. Wu, S. Burke, V. Viswanathan, *J. Electrochem. Soc.* **2019**, *166*, A4181–A4187.
- [27] A. Dave, J. Mitchell, K. Kandasamy, H. Wang, S. Burke, B. Paria, B. P'oczos, J. Whitacre, V. Viswanathan, *Cell Rep. Phys. Sci.* **2020**, *1*, 100264.
- [28] J. C. Burns, G. Jain, A. J. Smith, K. W. Eberman, E. Scott, J. P. Gardner, J. R. Dahn, *J. Electrochem. Soc.* **2011**, *158*, A255.
- [29] A. J. Smith, J. C. Burns, D. Xiong, J. R. Dahn, *J. Electrochem. Soc.* **2011**, *158*, A1136.
- [30] A. Weng, P. Mohtat, P. M. Attia, V. Sulzer, S. Lee, G. Less, A. Stefanopoulou, *Joule* **2021**, *5*, 2971–2992.
- [31] A. Yamaguchi, A. Omaru, M. Nagamine, M. Hasegawa, *Nonaqueous electrolyte secondary battery including vinylene carbonate and an antioxidant in the electrolyte*.
- [32] F. Sun, H. Markötter, I. Manke, A. Hilger, N. Kardjilov, J. Banhart, *ACS Appl. Mater. Interfaces* **2016**, *8*, 7156–7164.
- [33] L. D. Ellis, J. P. Allen, L. M. Thompson, J. E. Harlow, W. J. Stone, I. G. Hill, J. R. Dahn, *J. Electrochem. Soc.* **2017**, *164*, A3518–A3528.
- [34] C. Mao, R. E. Ruther, L. Geng, Z. Li, D. N. Leonard, H. M. Meyer, R. L. Sacci, D. L. Wood, *ACS Appl. Mater. Interfaces* **2019**, *11*, 43235–43243.
- [35] J. E. Harlow, X. Ma, J. Li, E. Logan, Y. Liu, N. Zhang, L. Ma, S. L. Glazier, M. M. E. Cormier, M. Genovese, S. Buteau, A. Cameron, J. E. Stark, J. R. Dahn, *J. Electrochem. Soc.* **2019**, *166*, A3031–A3044.
- [36] J. Snoek, H. Larochelle, R. P. Adams, *Practical Bayesian optimization of machine learning algorithms*. In *Advances in Neural Information Processing Systems*, **2012**, *25*, pages 2960–2968.
- [37] P. Hennig, C. J. Schuler, *J. Mach. Learn. Res.* **2012**, *13*, 1809–1837.
- [38] F. Nogueira, *Bayesian Optimization: Open source constrained global optimization tool for Python*, **2014**. <https://github.com/fmfn/BayesianOptimization>.

Manuscript received: January 21, 2022

Revised manuscript received: March 4, 2022

Accepted manuscript online: March 9, 2022

Version of record online: March 29, 2022